



Optimizing adhesive bonding between CFRP and Al alloy substrate through resin pre-coating by filling micro-cavities from sandblasting

Bo Tan^{a,b}, Yunsen Hu^b, Bingyan Yuan^b, Xiaozhi Hu^{b,*}, Zhaohui Huang^a

^a School of Materials Science and Technology, Beijing Key Laboratory of Materials Utilization of Nonmetallic Minerals and Solid Wastes, National Laboratory of Mineral Materials, China University of Geosciences, Beijing, 100083, PR China

^b Department of Mechanical Engineering, University of Western Australia, Perth, WA, 6009, Australia

ARTICLE INFO

Keywords:

CFRP
Al alloy substrate
Resin pre-coating (RPC)
Sandblasting
Shear strength

ABSTRACT

Strong adhesive bonding between carbon fibre reinforced polymer (CFRP) and aluminium (Al) alloy substrates is essential for structural integrity of modern aircrafts. This study reports a simple and effective method to increase the adhesion interface strength between CFRP and Al alloy substrates by means of a combined sandblasting and resin pre-coating (RPC) process. The RPC technique is used to maximize the full potential of surface abrasion from sandblasting by sealing all micro-cavities and wetting the entire surface and sub-surface openings over the Al substrate and CFRP. The RPC solution consisting of around 90 wt% of acetone and 10 wt% of resin (without hardener) takes resin into the surface micro-openings and effectively increases the wettability of bond surfaces. Based on single lap shear tests, over 170.2% of improvement in the shear strength has been achieved by the combined sandblasting and RPC method in compared with the adhesive joints without any surface treatment. The surface roughness, contact angle measurements and Scanning Electron Microscope (SEM) observations are conducted to investigate the wettability and microstructural details, confirming the effectiveness of the RPC technique.

1. Introduction

For complex structures such as aircraft, it is necessary to combine components of dissimilar materials, e.g. CFRP and light metals, using appropriate joining methods [1]. Compared with the traditional methods such as welding and bolt joint, adhesive bonding provides advantages of less weight, even distribution of the stress, water proofing and elimination of galvanic corrosion [2]. For this reason, it is mainly used for the interfacial bonding of larger-area surface between different parts in aircrafts [3]. Mostly for aircraft applications, CFRP is bonded directly to aluminium alloys in honeycomb sandwich construction. Titanium alloy is used for bonded joints to CFRP for most major load bearing applications. Considering the property variation across the interface and the consequent stress concentration, interfacial bond strength is crucial to structural performance between those dissimilar adherends [4].

The bond strength of an adhesive joint is linked to the adhesive strength and interfacial strengths between the adhesive joint and two substrates. While the adhesive strength is fixed for a given adhesive, the interfacial strengths with two substrates can still be tailored depending

on the substrate surface conditions, e.g. cleanness and micro-textures for possible mechanical interlocking of the polymer adhesive with the substrates [5]. Depending on the crack location and crack growth path inside the adhesive joint or at the interface, distinct failure modes have been defined [6]. (i) Adhesive failures indicate cracking along the bonding line between the adhesive and adherend/substrate. (ii) Cohesive failures occur within the adhesive layer, which is a common and preferred type of adhesive bond failure [7]. (iii) Mixed-mode failures of these two types are possible at different bond areas with characteristics of both adhesive and cohesive failures. (iv) Structural failures due to delamination in CFRP may occur if the overall bonding strength of an adhesive joint is higher than the peeling strength of laminar composite adherends [8].

This paper focus on the adhesive bonding between CFRP and Al alloy substrates, which are the two major materials with the largest consumptions in the modern aircraft. As shown in Fig. 1a and b, the original CFRP and Al alloy substrates both display a flat and smooth surface, although they are substantially different in hardness and material structures. Freshly abraded surfaces are often prepared for strong adhesive bonding, which can be explained by mechanical interlocking,

* Corresponding author.

E-mail address: xiao.zhi.hu@uwa.edu.au (X. Hu).

<https://doi.org/10.1016/j.ijadhadh.2021.102952>

Received 30 April 2021; Accepted 4 June 2021

Available online 8 July 2021

0143-7496/© 2021 Elsevier Ltd. All rights reserved.

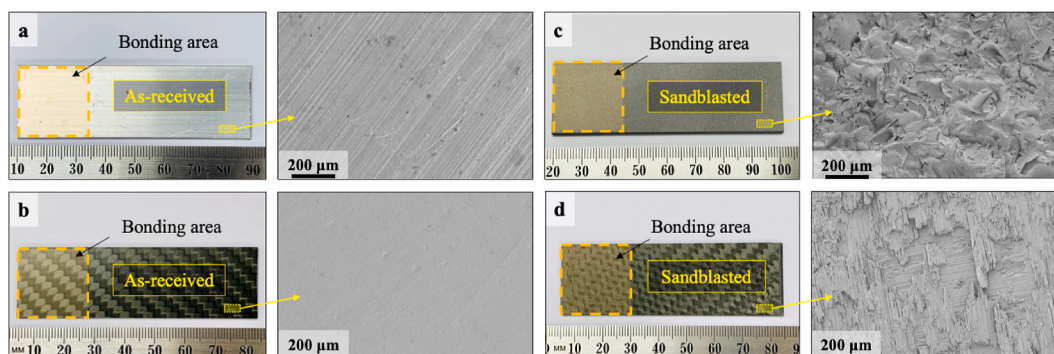


Fig. 1. Surface morphology images of Al alloy (a. as-received and c. sandblasted) and CFRP (b. as-received and d. sandblasted) substrates.

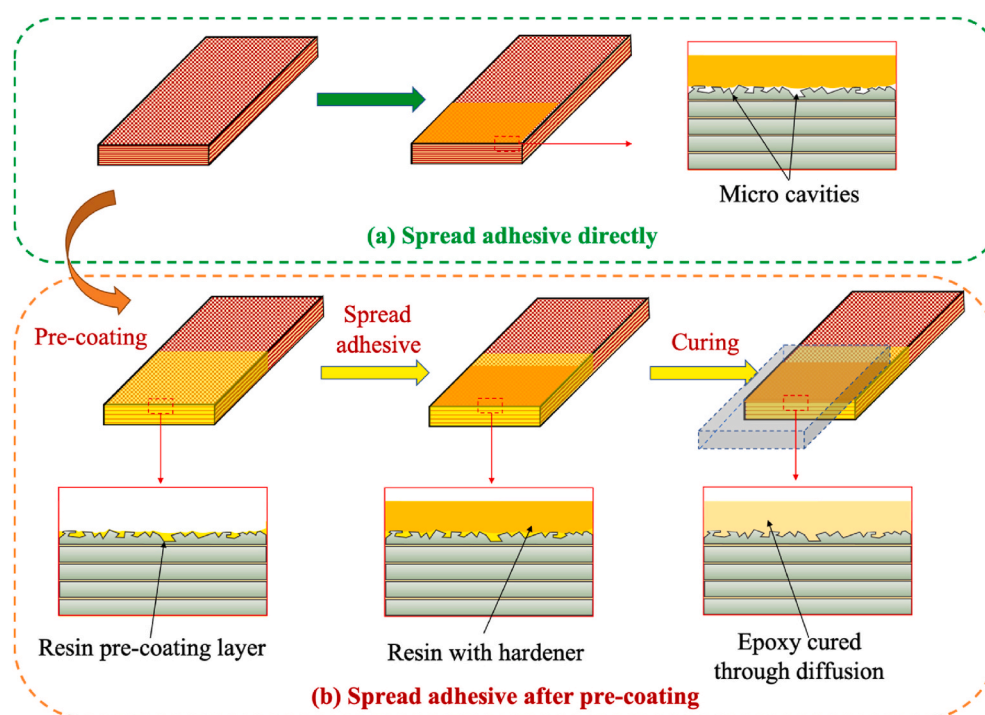


Fig. 2. (a) Normal adhesive bonding may not fill micro-cavities on the substrate surface. (b) Micro-cavities of the substrate surface are filled by the resin pre-coating (RPC) solution, and then followed by normal adhesive bonding.

increased surface area and surface wettability [9]. Clearly, surface pre-treatments of substrates are essential to the adhesive bond strength, and both physical (sandpaper polishing, sandblasting etc.) [10] and chemical methods (anodization etc.) [11] can be adopted. Based on the previous research, the RPC method may improve the wettability within the epoxy-metal (steel) [12] and epoxy-timber (jarrah wood) [8] interface. Jian et al. [13] have reported a 68.44% improvement of Al-Li alloy bonding strength based on the sandblasting technique after optimizing the treatment parameters. A moderate surface roughness is found to yield better wettability and stronger shear strength. Yunsen et al. [14] studied the influence of alkaline etching treatment method on the bonding strength of CFRP-Al adhesive joint and showed a maximum 91% improvement in bond strength after alkaline etching treatments.

According to the mechanical interlocking theory, adhesion occurs by the penetration of adhesives into cavities, pores, and other irregularities of the substrate rough surface. However, resins with high molecular weight and viscosity, or grits and occlusions from mechanical abrasion may prevent deep resin penetration. Therefore, a unique technique using acetone as a solvent to dilute the high-viscosity epoxy adhesive (without hardener) and promote the resin penetration into the rough

substrates surface, namely, resin pre-coating (RPC) was adopted in this study.

The RPC technique has been tested and found to be effective for bond strength enhancement of adhesive joints between metal (grit-blasted steel [15]), engineered bamboo [16] and granite [17] in previous studies. It will be adopted on the rough CFRP substrates for the first time in this study. As displayed in Fig. 2, the RPC solution containing acetone (70–90 wt%) and epoxy resin (10–30 wt%, with no hardener) can effectively penetrate into the bottoms of pits and gullies either from surface polishing/sanding where typically high-viscosity adhesives cannot flow into. After evaporation of acetone, the normal epoxy adhesive (resin with hardener) can be applied to join CFRP and Al alloy substrates. The pre-coated resin layer and adhesive will be cured simultaneously with the cross-linking process or diffusion of hardener. Finally, the epoxy adhesive layer between substrates can be deeply rooted into the rough Al and CFRP substrates, leading to much improved interfacial bond strength.

Table 1
The strength and curing time of Selleys Araldite Super Strength adhesive.

Strength ^a (MPa)	Setting time (h)	Initial bond time (h)	Max bond time (h)	Viscosity (Pa·s, 25 °C)		
				Part A	Part B	Mixed ^b
Up to 15	1–2	6–8	24–72	9.64	14.43	24.38

^a Holds up to 15 MPa when fully cured on steel.

^b The viscosity was tested during 5 min after mixing.

2. Experiment details

2.1. Materials

In this study, the commercially available 3 mm-thick 6060 T5 Al alloy flat bars from Midalia Steel Pty Ltd. (Perth, Western Australia) and the 2 mm-thick cross-ply [0/90]_{6s} CFRP sheets with 3 K twill weave outer layers made of T300 carbon fibres from CarbonWiz Technology Co., Ltd. (Shenzhen, China) were selected. They were cut into small pieces in dimension of 80 mm × 25 mm for substrates and 25 mm × 25 mm for shims to prepare single-lap joints. More detailed information about component and properties of Al alloy and CFRP can be found in the supplementary information.

A two-component epoxy resin adhesive named Selleys Araldite Super Strength Epoxy Adhesive (mainly bisphenol A epichlorohydrin epoxy resin and triethylenetetramine hardener, supplied by Dulux Group Pty

Ltd., Australia) for the adhesion and RPC processes (only the part of resin with no hardener). The basic properties are listed in Table 1. It can be used for load bearing repairs and is suitable for different kinds of materials such as metal, wood, plastic and glass [18]. Besides, Acetone was chosen for the surface cleaning of substrates and the preparation of RPC solution.

2.2. Surface cleaning and sandblasting

All the Al alloy and CFRP substrates were degreased in acetone solution assisted by ultrasound at room temperature for 45 min, then dried in air. The cleaned substrates were then sandblasted to obtain a rough surface finish under the following constant condition: Garnet grits in size of 30–60 μm in diameter, applied at the compressed air of 5 bars for 10 s per sample, the working distance was set to 100 mm, and sandblasting angle was decided to be 90° (the spray is perpendicular to the substrate surface). Sandblasting treatment was carried out by GMA Premium Blast machine (Perth, Australia) assisted by the UWA Engineering Faculty Workshop. The substrates were then ultrasound cleaned in acetone again for 45 min and dried in air at room temperature for 2 h.

As illustrated by Fig. 1c, the oxide layer on the Al alloy surface was removed by sandblasting, creating an uneven surface finish with micro-cavities. For CFRP substrates, sandblasting treatment could break the surface and sub-surface carbon fibre structures creating many micro-cracks and uneven surface features as displayed in Fig. 1d. It indicates that the sandblasting treatment is also effective for CFRP substrates to

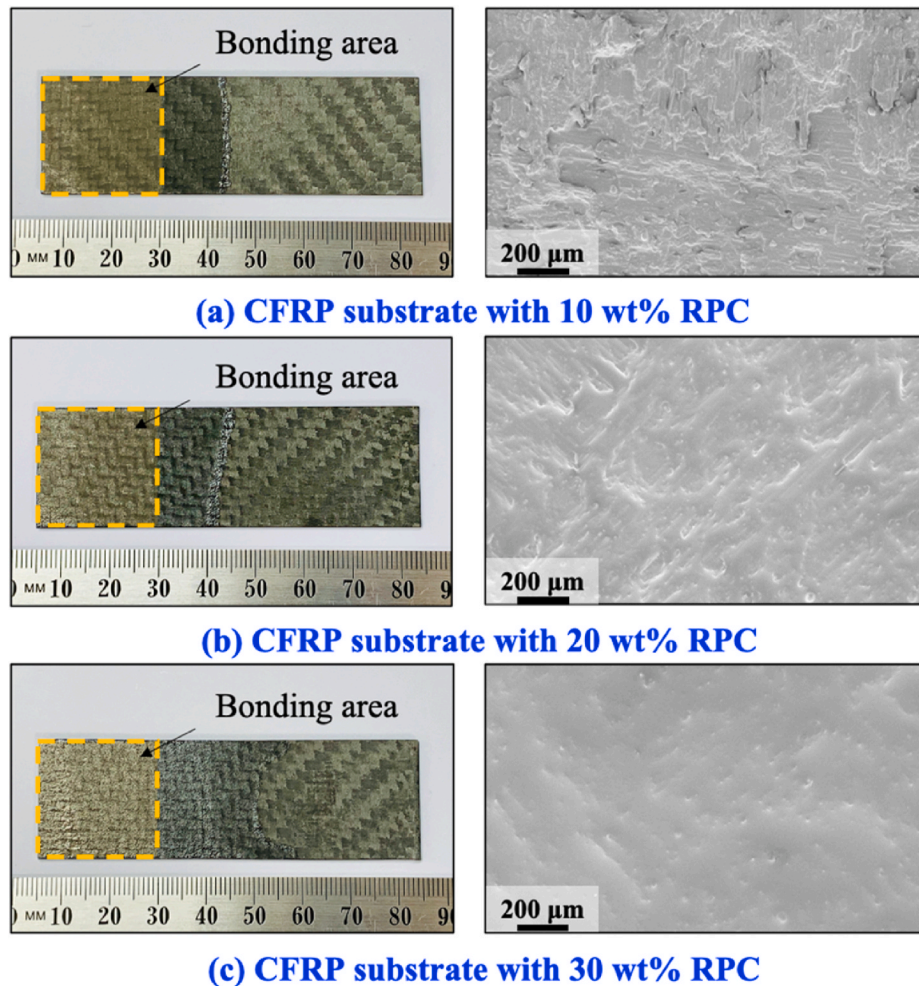


Fig. 3. Optical photographs and corresponding SEM images of CFRP substrates coated with RPC solutions of 10 wt% (a), 20 wt% (b) and 30 wt% (c) of resin (without hardener) in acetone. The SEM photos show the CFRP surface becomes smoother with the increasing resin wt%.

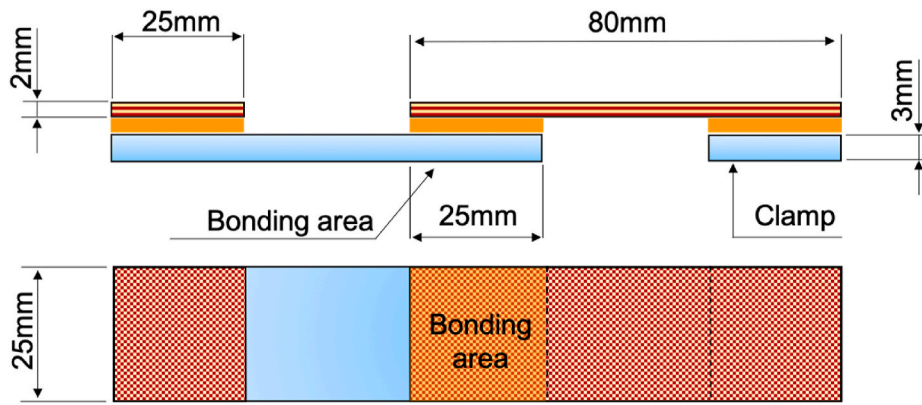


Fig. 4. SLS testing specimen dimension of the CFRP/Al joints.

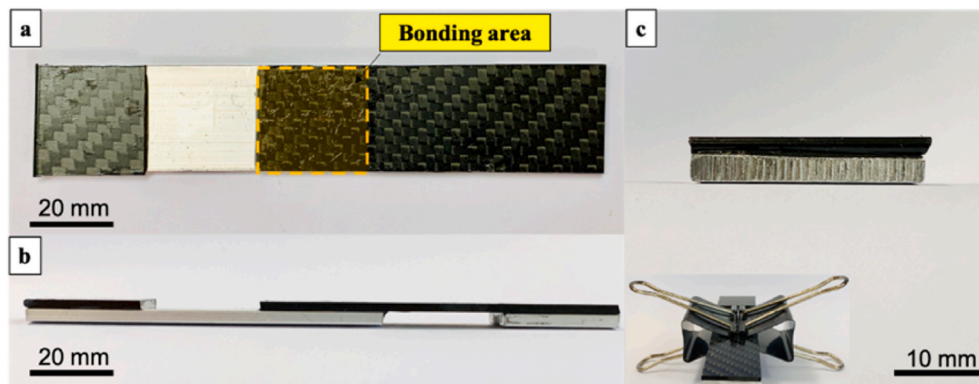


Fig. 5. Adhesive bonded CFRP/Al specimen for SLS test.

achieve an enhancement in surface roughness.

2.3. RPC (resin pre-coating) treatment

The acetone-rich RPC solution was prepared by dissolving a small wt % of resin part (without hardener) in acetone. For Al alloy substrates, the concentration of RPC solution was chosen to be 10 wt% of resin and 90 wt% of acetone based on the previous study [12]. Three RPC solutions with 10 wt%, 20 wt% and 30 wt% of resin were tried for the CFRP substrates. The RPC treatment was performed by dipping the substrates in the RPC solution for 10 s, and then dried in a fuming cupboard at room temperature for 30 min to let acetone evaporated completely. RPC can also be applied onto large areas by spraying or using a brush. Acetone evaporation is fast, which may not need 30 min.

The photos of substrates with RPC were shown in Fig. 3, where the pre-coated area for bonding appeared to be a little darker. As illustrated in the corresponding SEM images, the resin had penetrated into the microcracks on the roughened Al alloy and CFRP substrates surface. As schematically illustrated in Fig. 3a, b, and c, with the increase of the concentration of RPC solution, the surface profile of the rough CFRP substrates appeared smooth. It indicated that the residual amount of resin in increasing on the pre-coated CFRP substrates from 10 wt% to 30 wt%.

2.4. Experimental details

The surface roughness was determined by a profilometer (Altisurf 520, ALTIMET) via giving the value of Ra (Average Roughness) and Rq (Root Mean Square Roughness). The detailed definition of Ra and Rq can be found in the supplementary information. During the surface roughness measurement, three random starting points with a testing area of

Table 2

Surface treatment conditions of Al and CFRP substrates considered in this study.

Samples	Al alloy substrates		CFRP substrates	
	Sandblasting	RPC	Sandblasting	RPC
Control (un-treated)	–	–	–	–
P0 (sandblasting only)	Done	–	Done	–
P10	Done	10 wt%	Done	10 wt%
P20	Done	10 wt%	Done	20 wt%
P30	Done	10 wt%	Done	30 wt%

10 mm × 10 mm were set for each specimen. The average value of surface roughness parameters was recorded.

The wettability of adhesive on CFRP substrates with different surface conditions was investigated by contact angle measurement through a Dino Lite microscope. A drop (about 0.1 ml) of well-mixed two-part epoxy resin adhesive was placed onto the CFRP substrates using a syringe. The spreading process and contact angle of an epoxy drop on CFRP substrates were recorded by the microscope after 5s, 30s and 60s respectively.

The shear strength of the CFRP/Al joints was measured by the Single Lap Shear (SLS) testing method using an Instron 5982 mechanical testing machine. The specific dimension and the testing sample of the single-lap joints were displayed in Fig. 4 and Fig. 5 respectively. The bonding area was determined to be 25 mm × 25 mm according to the ASTM International standard (D5868). As shown in Fig. 5, all the glued specimens were pressed down by same spring clamps to maintain constant bonding area and squeeze out extra adhesive. The assembled joints were put in an air-dry oven for 20 min at 40 °C for primal shape setting firstly, and then 60 °C for 10 h for complete curing.

Specimens with five different surface treatment conditions as in

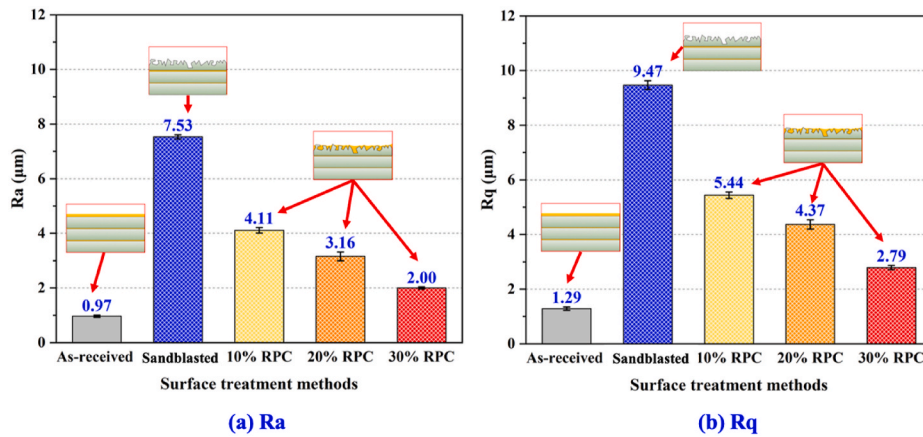


Fig. 6. Surface roughness parameters (a) Ra and (b) Rq of CFRP substrates by different surface treatments.

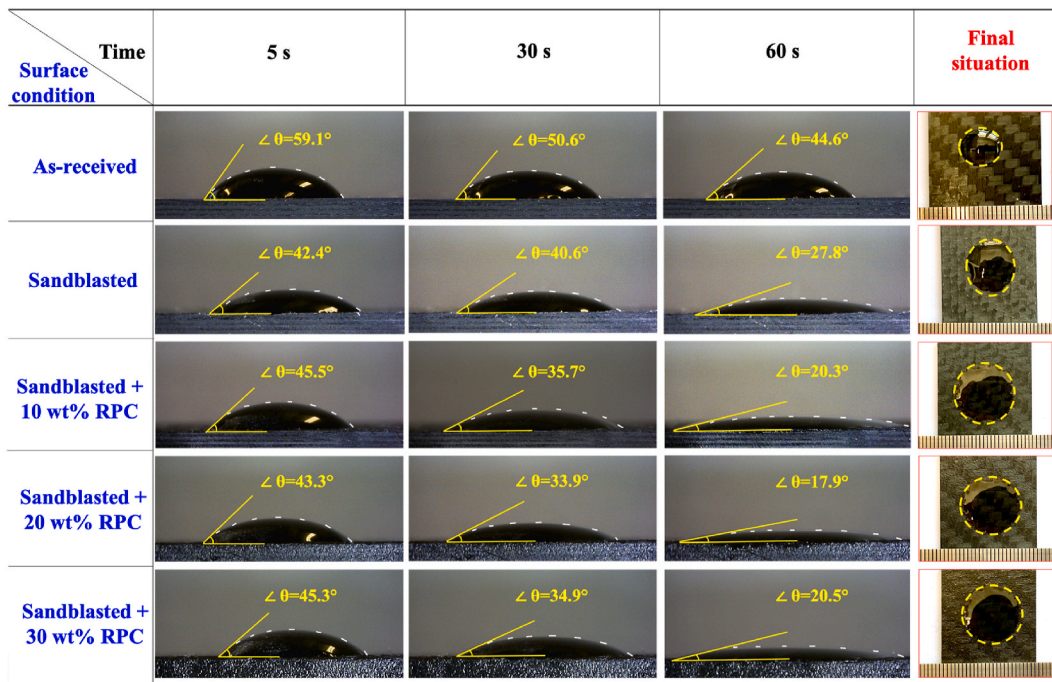


Fig. 7. Cross section view and final stable coverage areas by the epoxy droplets on CFRP substrates surface for contact angle measurements.

Table 2 were studied, i.e. Control, assembled by as-received Al alloy and CFRP substrates; P0, prepared by sandblasted Al alloy and CFRP substrates; P10, P20, and P30, fabricated by sandblasted Al alloy and CFRP substrates with RPC (the concentration of RPC solution for Al alloy substrates maintain 10 wt%, and the CFRP substrates were pre-coated by 10 wt%, 20 wt%, and 30 wt% of resin-acetone solution respectively). Five single-lap joints of each kind of specimens were tested, and the average values were calculated as the final results.

3. Results and discussion

3.1. Surface roughness analysis of CFRP substrates with different surface conditions

The average values and variation tendency of roughness parameters for CFRP substrates by different surface treatment are displayed in Fig. 6. Firstly, it can be found that the sandblasting enhanced the surface roughness of CFRP substrates significantly. The values of Ra and Rq are over seven times bigger than that before mechanical abrasion. Besides,

RPC technique changed the surface roughness towards an opposite tendency. The values of roughness parameters reduced as the increasing of RPC concentration. The sandblasted CFRP substrate pre-coated by 30 wt% of the resin-acetone solution gave the lowest value. Lower surface roughness means higher remaining amount of resin. Due to the RPC treatment, resin filled into the hollow of the roughened CFRP substrates which decreased the distance of “hills” and “valleys” on surface. The results of surface roughness analysis is consistent with the SEM observation in Figs. 1 and 3.

3.2. The influence of RPC method on wettability between adhesive and CFRP substrates

The effectiveness of the RPC technique on CFRP substrate was investigated in this study by contact angle test among six surface conditions, i.e. (1) as-received CFRP surface; (2) sandblasted CFRP surface; (3–5) sandblasted CFRP surface with 10 wt%, 20 wt% and 30 wt% of RPC treatment respectively.

Fig. 7 shows values of contact angle and the corresponding final

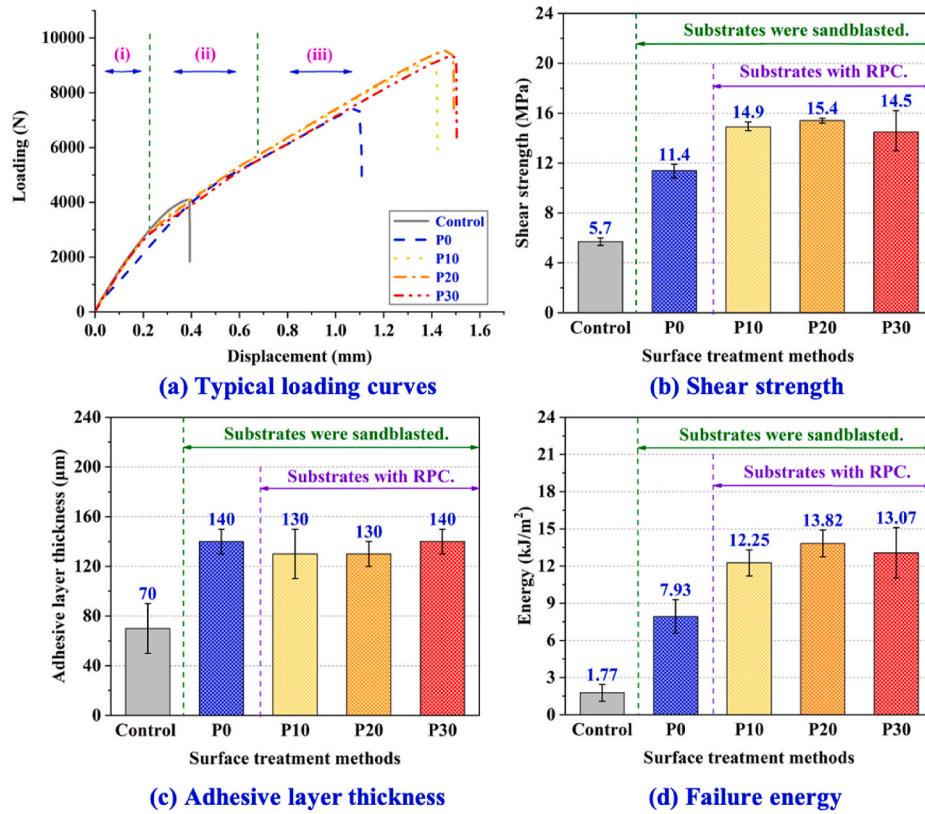


Fig. 8. Diagrams of (a) typical load-displacement curves, (b) shear strength values, (c) adhesive layer thickness values and (d) failure energy values for adhesive bonding samples by SLS testing.

coverage areas by the epoxy droplets. It appeared that the wettability of the CFRP substrates have been improved by the sandblasting treatment. It may be because the roughened surface with many empty pits and broken carbon fibre lead to capillary action so that the movement of the epoxy adhesive has been promoted. Compared with it on the as-received and only sandblasted CFRP surface, adhesive droplet showed lower contact angles and larger final coverage areas on those samples with RPC, which meant that the RPC technique led a further improvement in

wettability based on the sandblasting treatment. Besides, the concentration of the RPC solution showed little influence on the wettability. It indicated that the remaining resin had effectively filled in and covered the rough surface of the CFRP substrates after RPC treatment. Due to the remaining epoxy layer with similar adhesive component on the CFRP substrates surface from RPC technique, the wettability was improved.

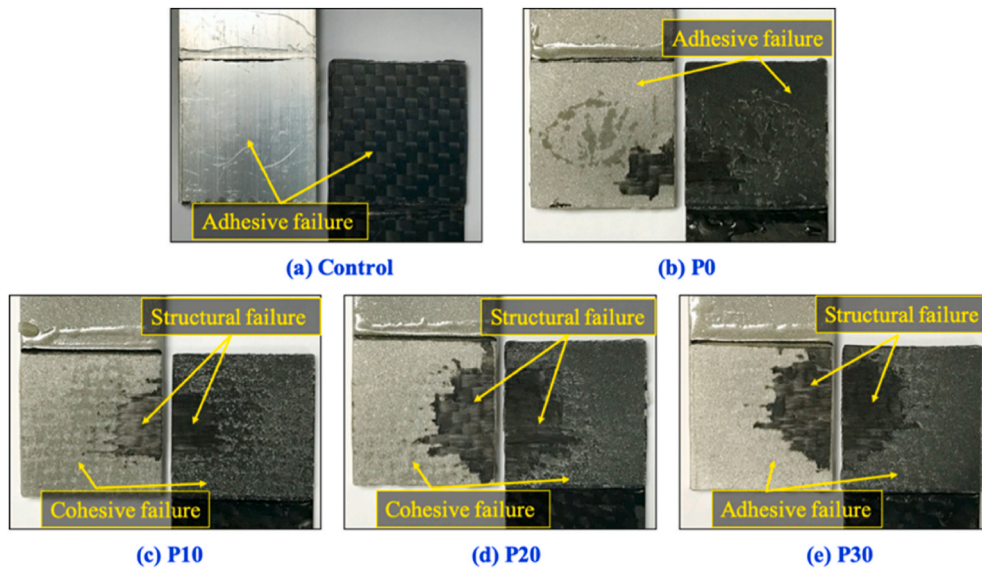


Fig. 9. Sheared failure interface images of (a) Control, as-received substrates; (b) P0, sandblasting only; (c) P10, CFRP substrates with 10 wt% RPC; (d) P20, CFRP substrates with 20 wt% RPC; (e) P30, CFRP substrates with 30 wt% RPC.

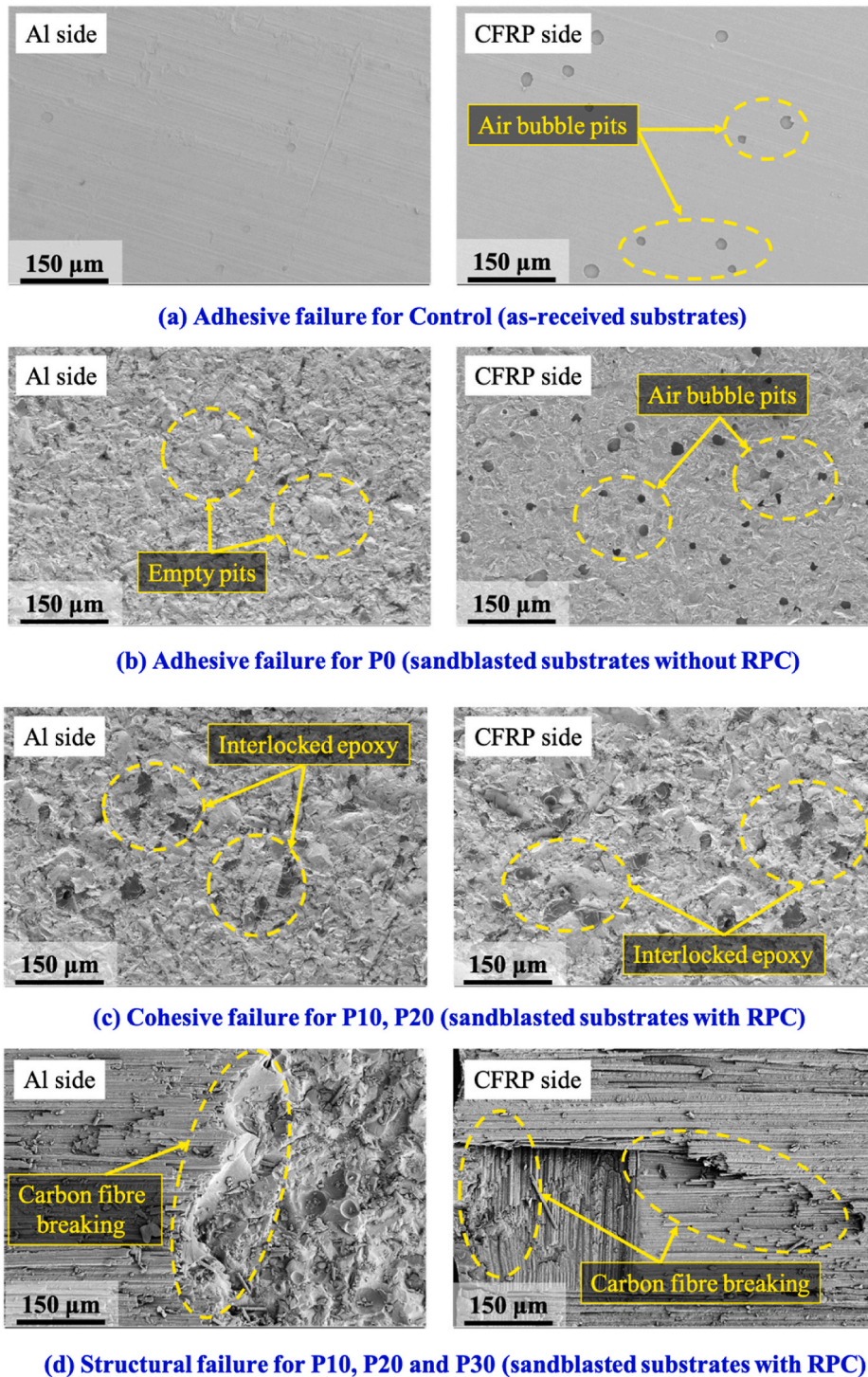


Fig. 10. SEM images of typical failure modes on sheared Al alloy and CFRP substrates surface with and without RPC.

3.3. The effects of RPC (resin pre-coating) on bonding strength

SLS tests were carried out using an Instron 5982 mechanical testing machine in 100 KN load range with the displacement rate of 1 mm/min. Detailed test results of five single-lap joints were listed in the supplementary information.

The typical loading-displacement curves were displayed in Fig. 8a. The shear failure process can be divided into three stages: (I) the initial failure stage associated with elastic deformation of epoxy adhesive; (II) the non-linear failure stage associated with epoxy plastic deformation

and interface debonding; (III) the elastic failure stage caused by the epoxy cohesive failure and structure failure. Increase in the peak loads was mainly benefited from the elongated region of (III) for samples [11]. That is both the peak load and energy absorption were increased.

The varying trend of average shear strength and adhesive layer thickness were displayed in Fig. 8b and c respectively. It can be found that an obvious improvement in bonding strength was achieved by sandblasting treatment. P0 displayed average shear strength value of 11.4 MPa which showed 100.0% improvement from 5.7 MPa of Control. Besides, the adhesive layer thickness of joint has been enhanced for

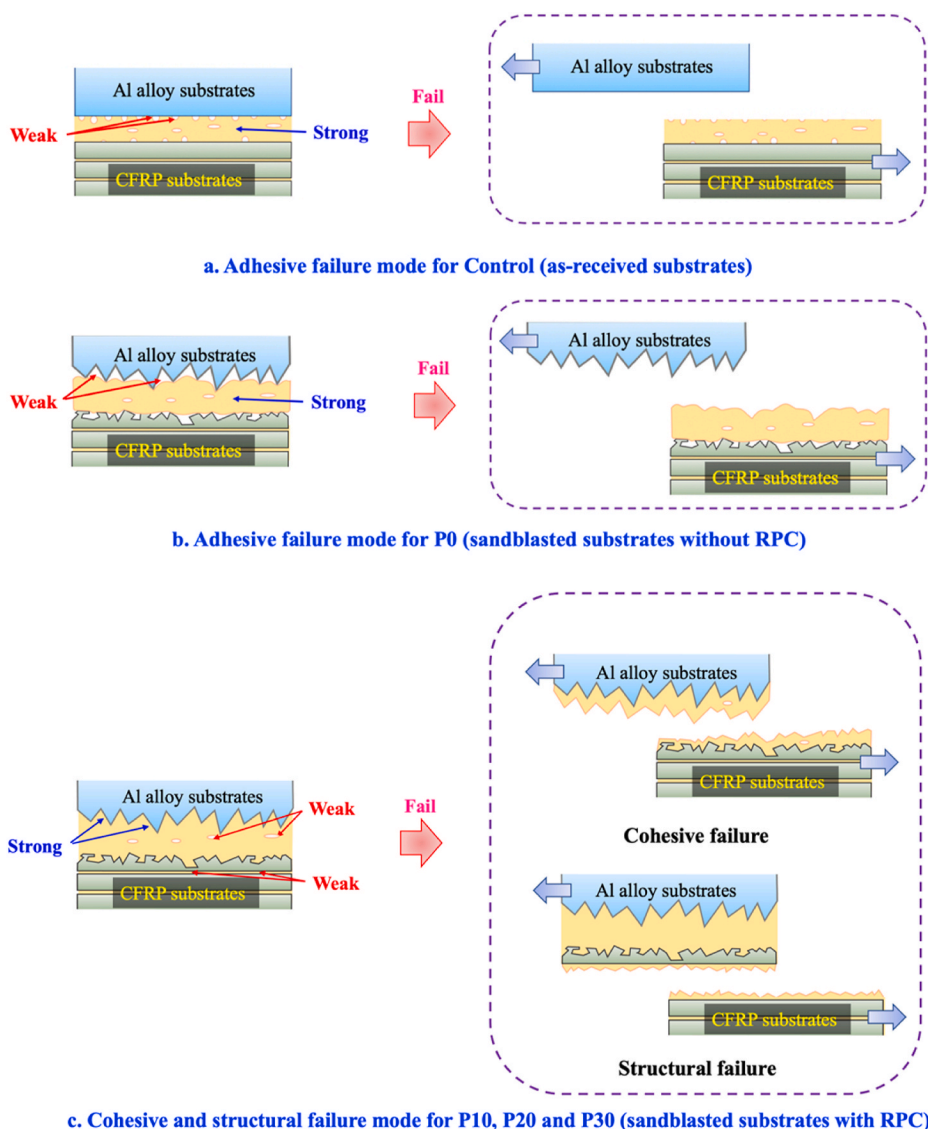


Fig. 11. Schematic of typical failure mode of CFRP/Al alloy adhesive joints with/without RPC.

double from Control to P0 as well. It indicated that the sandblasting method not only roughened the substrate surface leading to a stronger interlocking capability, but also the total contact area between the sandblasted substrates and adhesive was increased.

Moreover, compared with the P0 samples, all the RPC-treated samples showed over 30% improvement in the shear strength. P20 had the highest shear strength values of 15.4 MPa, which showed an extra improvement of 35.1% from 11.4 MPa of P0. P10 and P30 displayed similar average shear strength values of 14.9 MPa and 14.5 MPa, respectively. In contrast with the Control, the total increase in shear strength of P10, P20, and P30 achieved 161.4%, 170.2%, and 154.4%, respectively. It showed a similar trend for failure energy values in Fig. 8d. P20 gave the highest values of 13.82 kJ/m² which showed a total enhancement of 680.8% from that of Control.

3.4. Failure patterns observation and reinforcement mechanisms analysis

The sheared surface of the five single-lap joints were displayed in Fig. 9. Almost the whole adhesive layer was peeled off and remained on the CFRP substrate for the joint without any surface treatment in Fig. 9a. The corresponding microstructure of the adhesive failure area was shown in Fig. 10a. The smooth shear-failure surface of the adhesive on

CFRP exposed many air bubble empty pits. Due to the poor wettability between the original substrates and adhesive, cracks growth along the interface between Al alloy substrate and adhesive layer which displayed adhesive failure mode as in Fig. 11a.

Besides, it was found that adhesive failure also occurred predominantly within the sheared surface of P0 (sandblasted substrates without RPC) as in Fig. 9b. Fig. 10b showed the SEM observation of the adhesive failure area. Micro-pores without interlocked epoxy were observed. It indicated that although the rough surface led to stronger interlocking and gave an enhancement in bonding strength, the adhesive did not wet the substrates and fill into those micro-pits completely. Thus, as illustrated in Fig. 11b, the P0 displayed the adhesive failure mode mainly at the metal/adhesive interface.

A noticeable structural failure area along the sheared substrates surface can be observed in the RPC-treated cases of RPC treated, as shown in Fig. 9c–e. With the increasing resin concentration, P20 showed a large structural failure area and gave the highest shear strength. The rest area of sheared surface was mainly covered by cohesive failure for P10 and P20. Fig. 10c displayed the microstructure of the typical cohesive failure area. There were no visible micro-pores and pits. On the contrary, many interlocked epoxy sites embedded on the sheared surface. It showed that, due to the RPC method, epoxy resin can fully

penetrate deep into the micro-cavities and fissures created by sandblasting and lead to a stronger bonding strength between the interface of substrates and adhesive layer. The fracture occurred within the internal structure of adhesive layer and displayed cohesive failure as in Fig. 11c. For the structural failure area in Fig. 9c–e, many carbon fibres breaking can be found in corresponding SEM images of Fig. 10d. It suggested that the acetone has taken resin into the internal structure of CFRP substrates. The thin adhesive layer was further rooted into the porous CFRP substrate and produced high bonding strength, thus the failure would be transferred into the internal structure of CFRP substrates displayed structural failure.

It shall be mentioned that the concentration of RPC solution for CFRP substrates should not be too high. Among the samples with RPC, P30 gave a lower shear strength than P20 and the sheared surface was covered by adhesive failure area partly as in Fig. 9e. It may be because that the hardener in the final mixed two-part epoxy is insufficient for diffusion and curing of the RPC region with such a large amount of resin in P30 completely. Therefore, 20 wt% would be the most appropriate RPC solution concentration for the rough CFRP substrates.

4. Conclusions

This study shows that sandblasting commonly-used for surface preparation of various substrates can be made more effective by the simple resin pre-coating (RPC) method before normal adhesive bonding. Based on the SLS testing results, the shear strength has been improved by at least 30% by applying RPC before normal adhesive bonding. The maximum shear strength improvement in the shear strength was as high as 170%, considering the combined effects of sandblasting and RPC.

Similar to sandblasting, RPC can be conveniently applied on site through either spraying or blushing. There is no other chemical involved, and the evaporation of acetone after RPC is fast. The significantly enhanced energy absorption ability and critical displacement at fracture as in Fig. 8a and d shows the adhesive joints with RPC are more damage resistant than the common adhesive joints without RPC. Elimination of micro-air pockets in micro-cracks and cavities on substrate surfaces and wetting the substrate surface are the main functions of RPC. With the help of RPC, the adhesive joint is able to penetrate deeply into micro-cavities on the substrate surfaces forming multiple micro-roots after the RPC-filled resin is cured.

Acknowledgements

The authors acknowledge for the financial support from the China Scholarship Council (201606400039), and the technical assistance of X-ray tomography and SEM analysis from the UWA Centre of Microscopy, Characterization & Analysis, and the assistance in sample preparation from UWA Engineering Faculty Workshop.

Appendix A. Supplementary data

Supplementary data to this article can be found online at <https://doi.org/10.1016/j.ijadhadh.2021.102952>.

[org/10.1016/j.ijadhadh.2021.102952](https://doi.org/10.1016/j.ijadhadh.2021.102952).

References

- [1] Custódio J, Broughton J, Cruz H. A review of factors influencing the durability of structural bonded timber joints. *Int J Adhesion Adhes* 2009;29(2):173–85. <https://doi.org/10.1016/j.ijadhadh.2008.03.002>.
- [2] Adams RD, Comyn J, Wake WC. *Structural adhesive joints in engineering*. London: Chapman & Hall; 1997.
- [3] Zimmermann N, Wang PH. A review of failure modes and fracture analysis of aircraft composite materials. *Eng Fail Anal* 2020;115:104692. <https://doi.org/10.1016/j.engfailanal.2020.104692>.
- [4] Kumar P, Patnaik A, Chaudhary S. A review on application of structural adhesives in concrete and steel–concrete composite and factors influencing the performance of composite connections. *Int J Adhesion Adhes* 2017;77:1–14. <https://doi.org/10.1016/j.ijadhadh.2017.03.009>.
- [5] Wong DWY, Zhang H, Bilotti E, Peijs T. Interlaminar toughening of woven fabric carbon/epoxy composite laminates using hybrid aramid/phenoxy interleaves. *Compos Part A Appl Sci Manuf* 2017;101:151–9. <https://doi.org/10.1016/j.compositesa.2017.06.001>.
- [6] Brandtner-Hafner M. Interface fracture mechanics of notched wood-adhesive composites and mode I, II, III loading. *Int Symp Notch Fract* 2017;4:29–31. <https://www.researchgate.net/publication/315833570>.
- [7] Weißgraeber P, Becker W. Finite Fracture Mechanics model for mixed mode fracture in adhesive joints. *Int J Solid Struct* 2013;50:2383–94. <https://doi.org/10.1016/j.ijsolstr.2013.03.012>.
- [8] Tan B, Ji Y, Hu Y, Yuan B, Hu X, Huang Z. Pretreatment using diluted epoxy adhesive resin solution for improving bond strength between steel and wood surfaces. *Int J Adhesion Adhes* 2019;3–10. <https://doi.org/10.1016/j.ijadhadh.2019.102502>.
- [9] Fernando D, Teng JG, Yu T, Zhao XL. Preparation and characterization of steel surfaces for adhesive bonding. *J Compos Construct* 2013;17:1–10. [https://doi.org/10.1061/\(ASCE\)CC.1943-5614.0000387](https://doi.org/10.1061/(ASCE)CC.1943-5614.0000387).
- [10] Lim AS, Melrose ZR, Thostenson ET, Chou TW. Damage sensing of adhesively-bonded hybrid composite/steel joints using carbon nanotubes. *Compos Sci Technol* 2011;71:1183–9. <https://doi.org/10.1016/j.compscitech.2010.10.009>.
- [11] He P, Chen K, Yu B, Yue CY, Yang J. Surface microstructures and epoxy bonded shear strength of Ti₆Al₄V alloy anodized at various temperatures. *Compos Sci Technol* 2013;82:15–22. <https://doi.org/10.1016/j.compscitech.2013.04.007>.
- [12] Wang B, Bai Y, Hu X, Lu P. Enhanced epoxy adhesion between steel plates by surface treatment and CNT/short-fibre reinforcement. *Compos Sci Technol* 2016;127:149–57. <https://doi.org/10.1016/j.compscitech.2016.03.008>.
- [13] Li J, Li Y, Huang M, Xiang Y, Liao Y. Improvement of aluminum lithium alloy adhesion performance based on sandblasting techniques. *Int J Adhesion Adhes* 2018;84:307–16. <https://doi.org/10.1016/j.ijadhadh.2018.04.007>.
- [14] Hu Y, Yuan B, Cheng F, Hu X. NaOH etching and resin pre-coating treatments for stronger adhesive bonding between CFRP and aluminium alloy. *Compos B Eng* 2019;178:107478. <https://doi.org/10.1016/j.compositesb.2019.107478>.
- [15] Wang B, Hu X, Lu P. Improvement of adhesive bonding of grit-blasted steel substrates by using diluted resin as a primer. *Int J Adhesion Adhes* 2017;73:92–9. <https://doi.org/10.1016/j.ijadhadh.2016.11.012>.
- [16] Liu W, Zheng Y, Hu X, Han X, Chen Y. Interfacial bonding enhancement on the epoxy adhesive joint between engineered bamboo and steel substrates with resin pre-coating surface treatment. *Wood Sci Technol* 2019;53:785–99. <https://doi.org/10.1007/s00226-019-01109-9>.
- [17] Han X, Yuan B, Tan B, Hu X, Chen S. Repair of subsurface micro-cracks in rock using resin pre-coating technique. *Construct Build Mater* 2019;196:485–91. <https://doi.org/10.1016/j.conbuildmat.2018.11.145>.
- [18] Selleys. The product introduction of Selleys araldite super strength adhesive. 2019. <http://www.selleys.com.au/adhesives/household-adhesive/araldite/super-strength/#information>.